UH-511-864-96
ISU-HET-97-05
May 1997

CP Violation in Quasi-inclusive $B \to K^{(*)}X$ Decays

T. E. Browder[1], A. Datta[2], X.-G. He[3] and S. Pakvasa[1]

[1] *Department of Physics and Astronomy*
University of Hawaii,
Honolulu, Hawaii 96822
[2] *Department of Physics and Astronomy*
Iowa State University,
Ames, Iowa 50011
And
[3] *School of Physics*
University of Melbourne,
Parkville, Victoria, 3052
Australia

Abstract

We consider the possibility of observing CP violation in quasi-inclusive decays of the type $B^- \to K^- X$, $B^- \to K^{*-} X$, $\bar{B}^0 \to K^- X$ and $\bar{B}^0 \to K^{*-} X$, where X does not contain strange quarks. We present estimates of rates and asymmetries for these decays in the Standard Model and comment on the experimental feasibility of observing CP violation in these decays at future B factories. We find the rate asymmetries can be quite sizeable.

I. INTRODUCTION

The possibility of observing large CP violating asymmetries in the decay of B mesons motivates the construction of high luminosity B factories at several of the world's high energy physics laboratories. The theoretical and the experimental signatures of these asymmetries have been extensively discussed elsewhere [1], [2], [3], [4], [5]. At asymmetric B factories, it is possible to measure the time dependence of B decays and therefore time dependent rate asymmetries of neutral B decays due to $B-\bar{B}$ mixing. The measurement of time dependent asymmetries in the exclusive modes $\bar{B}^0 \to \psi K_s$ and $\bar{B}^0 \to \pi^+\pi^-$ will allow the determination of the angles in the Cabbibo-Kobayashi-Maskawa unitarity triangle. This type of CP violation has been studied extensively in the literature.

Another type of CP violation also exists in B decays, direct CP violation in the B decay amplitudes. This type of CP violation in B decays has also been discussed by several authors although not as extensively. For charged B decays calculation of the magnitudes of the effects for some exclusive modes and inclusive modes have been carried out [6], [7], [8], [9], [10], [11], [12]. In contrast to asymmetries induced by $B-\overline{B}$ mixing, the magnitudes have large hadronic uncertainties, especially for the exclusive modes. Observation of these asymmetries can be used to rule out the superweak class of models [13].

In this paper we describe several quasi-inclusive experimental signatures which could provide useful information on direct CP violation at the high luminosity facilities of the future. One of the goals is to increase the number of events available at experiments for observing a CP asymmetry. In particular we examine the inclusive decay of the neutral and the charged B to either a charged K or a charged K^* meson. By applying the appropriate cut on the kaon (or K^*) energy one can isolate a signal with little background from $b \to c$ transitions. Furthermore, these quasi-inclusive modes are expected to have less hadronic uncertainty than the exclusive modes, would have larger branching ratios and, compared to the purely inclusive modes they may have larger CP asymmetries. In this paper we will consider modes of the type $B \to K(K^*)X$ that have the strange quark only in the $K(K^*)$-meson.

In the sections which follow, we describe the experimental signature and method. We then calculate the rates and asymmetries for inclusive $B^- \to K^-(K^{*-})$ and $\bar{B}^0 \to K^-(K^{*-})$ decays. In the last section the theoretical uncertainties in the calculation are discussed.

II. EXPERIMENTAL SIGNATURES FOR QUASI-INCLUSIVE $B \to SG^*$

In the $\Upsilon(4S)$ center of mass frame, the momentum of the $K^{(*)-}$ from quasi-two body B decays such as $B \to K^{(*)-}X$ may have momenta above the kinematic limit for $K^{(*)-}$ mesons from $b \to c$ transitions. This provides an experimental signature for $b \to sg^*$, $g^* \to u\bar{u}$ or $g^* \to d\bar{d}$ decays where g^* denotes a gluon. This kinematic separation between $b \to c$ and $b \to sg^*$ transitions is illustrated by a generator level Monte Carlo simulation in Figure 1 for the case of $B \to K^{*-}$. (The $B \to K^-$ spectrum will be similiar). This experimental signature can be applied to the asymmetric energy B factories if one boosts backwards along the z axis into the $\Upsilon(4S)$ center of mass frame.

Since there is a large background ("continuum") from the non-resonant processes $e^+e^- \to q\bar{q}$ where $q = u, d, s, c$, experimental cuts on the event shape are also imposed. To provide additional continuum suppression, the "B reconstruction" technique has been employed. The requirement that the kaon and n other pions form a system consistent in beam constrained mass and energy with a B meson dramatically reduces the background. After these requirements are imposed, one searches for an excess in the kaon momentum spectrum above the $b \to c$ region. Only one combination per event is chosen. No effort is made to unfold the feed-across between submodes with different values of n.

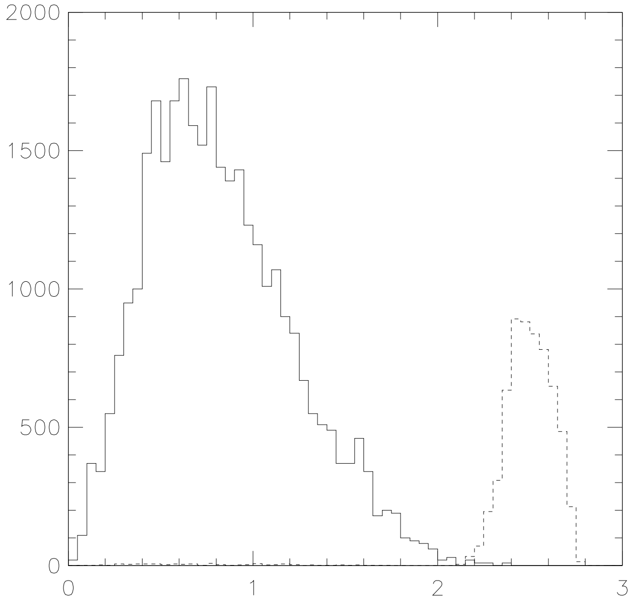

FIG. 1. Generated Inclusive $B \to K^{*-}$ momentum spectrum. The component below 2.0 GeV/c is due to $b \to c$ decays while the component above 2.0 GeV/c arises from quasi-two body $b \to sg^*$ decay. The normalization of the $b \to c$ component is reduced by a factor of approximately 100 so that both components are visible.

Methods similar to these have been successfully used by the CLEO II experiment to isolate a signal in the inclusive single photon energy spectrum and measure the branching fraction for inclusive $b \to s\gamma$ transitions and to set upper limits on $b \to s\phi$ transitions [14], [15]. It is clear from these studies that the B reconstruction method provides adequate continuum background suppression.

The decay modes that will be used here are listed below:

1. $B^- \to K^{(*)-}\pi^0$
2. $\bar{B}^0 \to K^{(*)-}\pi^+$
3. $B^- \to K^{(*)-}\pi^-\pi^+$

4. $\bar{B}^0 \to K^{(*)-}\pi^+\pi^0$

5. $\bar{B}^0 \to K^{(*)-}\pi^+\pi^-\pi^+$

6. $B^- \to K^{(*)-}\pi^+\pi^-\pi^0$

7. $B^- \to K^{(*)-}\pi^+\pi^-\pi^+\pi^-$

8. $\bar{B}^0 \to K^{(*)-}\pi^+\pi^-\pi^+\pi^0$

In case of multiple entries for a decay mode, we choose the best entry on the basis of a χ^2 formed from the beam constrained mass and energy difference (i.e. $\chi^2 = (M_B/\delta M_B)^2 + (\Delta E/\delta\Delta E)^2$). In case of multiple decay modes per event, the best decay mode candidate is picked on the basis of the same χ^2.

Cross-feed between different $b \to sg$ decay modes (i.e. the misclassification of decay modes) provided the $K^{(*)-}$ is correctly identified, is not a concern as the goal is to extract an inclusive signal. The purpose of the B reconstruction method is to reduce continuum background. As the multiplicity of the decay mode increases, however, the probability of misrecontruction will increase.

The signal is isolated as excess $K^{(*)-}$ production in the high momentum signal region ($2.0 < p_{K^{(*)}} < 2.7$ GeV) above continuum background. To reduce contamination from high momentum $B \to \pi^-(\rho^-)$ production and residual $b \to c$ background, we assume the presence of a high momentum particle identification system as will be employed in the BABAR, BELLE, and CLEO III experiments.

We propose to measure the asymmetry $N(K^{(*)+} - K^{(*)-})/N(K^{(*)+} + K^{(*)-})$ where $K^{(*)\pm}$ originates from a partially reconstructed B decay such as $B \to K^{(*)-}(n\pi)^0$ where the additional pions have net charge 0 and $n \leq 4$ and one neutral pion is allowed and $2.7 > p(K^{(*)-}) > 2.0$ GeV. We assume that the contribution from $B \to K^-\eta^{'}X$ decays has been removed by cutting on the $\eta^{'}$ region in X mass. It is possible that the anomalously large rate from this source [16] could dilute the asymmetry.

III. EFFECTIVE HAMILTONIAN

In the Standard Model (SM) the amplitudes for hadronic B decays of the type $b \to q\bar{f}f$ are generated by the following effective Hamiltonian [17]:

$$H_{eff}^q = \frac{G_F}{\sqrt{2}}[V_{fb}V_{fq}^*(c_1O_{1f}^q + c_2O_{2f}^q) - \sum_{i=3}^{10}(V_{ub}V_{uq}^*c_i^u + V_{cb}V_{cq}^*c_i^c + V_{tb}V_{tq}^*c_i^t)O_i^q] + H.C. \,, \tag{1}$$

where the superscript u, c, t indicates the internal quark, f can be u or c quark. q can be either a d or a s quark depending on whether the decay is a $\Delta S = 0$ or $\Delta S = -1$ process. The operators O_i^q are defined as

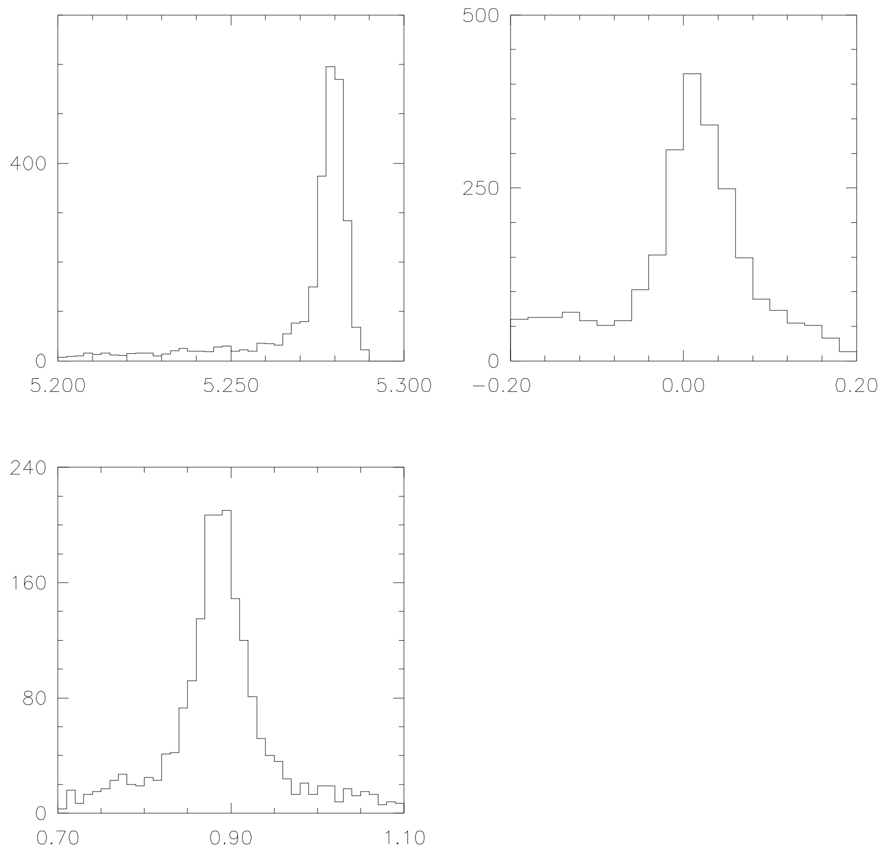

FIG. 2. Monte Carlo simulation of inclusive $B \to K^{*-}X$ signal with the B reconstruction method: (a) The beam constrained mass distribution (b) The distribution of energy difference (c) The $K^-\pi^0$ invariant mass after selecting on energy difference and beam constrained mass

$$
\begin{aligned}
&O^q_{f1} = \bar{q}_\alpha \gamma_\mu L f_\beta \bar{f}_\beta \gamma^\mu L b_\alpha \ , \qquad O^q_{2f} = \bar{q}\gamma_\mu L f \bar{f} \gamma^\mu L b \ , \\
&O^q_{3,5} = \bar{q}\gamma_\mu L b \bar{q}' \gamma_\mu L(R) q' \ , \qquad O^q_{4,6} = \bar{q}_\alpha \gamma_\mu L b_\beta \bar{q}'_\beta \gamma_\mu L(R) q'_\alpha \ , \\
&O^q_{7,9} = \frac{3}{2}\bar{q}\gamma_\mu L b e_{q'} \bar{q}' \gamma^\mu R(L) q' \ , \ O^q_{8,10} = \frac{3}{2}\bar{q}_\alpha \gamma_\mu L b_\beta e_{q'} \bar{q}'_\beta \gamma_\mu R(L) q'_\alpha \ ,
\end{aligned} \tag{2}
$$

where $R(L) = 1 \pm \gamma_5$, and q' is summed over u, d, and s. O_1 and O_2 are the tree level and QCD corrected operators. O_{3-6} are the strong gluon induced penguin operators, and operators O_{7-10} are due to γ and Z exchange (electroweak penguins), and "box" diagrams at loop level. The Wilson coefficients c_i^f are defined at the scale $\mu \approx m_b$ and have been evaluated to next-to-leading order in QCD. The c_i^t are the regularization scheme independent values obtained in Ref. [9]. We give the non-zero c_i^f below for $m_t = 176$ GeV, $\alpha_s(m_Z) = 0.117$, and $\mu = m_b = 5$ GeV,

$$
\begin{aligned}
&c_1 = -0.307 \ , \ \ c_2 = 1.147 \ , \ \ c_3^t = 0.017 \ , \ \ c_4^t = -0.037 \ , \ \ c_5^t = 0.010 \ , c_6^t = -0.045 \ , \\
&c_7^t = -1.24 \times 10^{-5} \ , \ \ c_8^t = 3.77 \times 10^{-4} \ , \ \ c_9^t = -0.010 \ , \ \ c_{10}^t = 2.06 \times 10^{-3} \ ,
\end{aligned}
$$

$$c_{3,5}^{u,c} = -c_{4,6}^{u,c}/N_c = P_s^{u,c}/N_c \ , \quad c_{7,9}^{u,c} = P_e^{u,c} \ , \quad c_{8,10}^{u,c} = 0 \tag{3}$$

where N_c is the number of color. The leading contributions to $P^i_{s,e}$ are given by: $P^i_s = (\frac{\alpha_s}{8\pi})c_2(\frac{10}{9} + G(m_i, \mu, q^2))$ and $P^i_e = (\frac{\alpha_{em}}{9\pi})(N_c c_1 + c_2)(\frac{10}{9} + G(m_i, \mu, q^2))$. The function $G(m, \mu, q^2)$ is given by

$$G(m, \mu, q^2) = 4\int_0^1 x(1-x)\ln\frac{m^2 - x(1-x)q^2}{\mu^2}\, \mathrm{d}x \ . \tag{4}$$

All the above coefficients are obtained up to one loop order in electroweak interactions. The momentum q is the momentum carried by the virtual gluon in the penguin diagram. When $q^2 > 4m^2$, $G(m, \mu, q^2)$ becomes imaginary. In our calculation, we use $m_u = 5$ MeV, $m_d = 7$ MeV, $m_s = 200$ MeV, $m_c = 1.35$ GeV [18,19].

We assume that the final state phases calculated at the quark level will be a good approximation to the sizes and the signs of the FSI phases at the hadronic level for quasi-inclusive decays when the final state particles are quite energetic as is the case for the B decays in the kinematic range of experimental interest [6]. As pointed out by Gerard and Hou [7] and clarified by Wolfenstein [8]. when calculating rate asymmetries using the absorptive amplitude given above, one must be careful to be consistent with the requirements of the CPT theorem. Gerard and Hou [7] noted that CPT is violated if one does not include all diagrams of the same order. The interference term responsible for rate asymmetry due to ${c_i}^u$ contains two contributions: an interference between penguin amplitudes of order ${\alpha_s}^2$ and a contribution from the interference of the tree amplitude with a higher order penguin diagram that contains an absorptive part from a vacuum polarization bubble in the gluon propagator. These two contributions cancel each other. Therefore, in practical calculations ${c_i}^u$ must be treated as real. The general rule is that the phase of the penguin Wilson coefficient must be dropped if there is a tree amplitude with the same CKM factor and the final states for the tree and the penguin amplitude are the same. In a more general analysis of this problem from CPT and unitarity consideration [8], Wolfenstein showed that diagonal strong phases (the phases due to the rescattering of the state which is the same as the final state e.g. $u\bar{u} \to u\bar{u}$) do not contribute to partial rate asymmetry. The phase in ${c_i}^u$ is a diagonal phase in this sense. We will follow this prescription of Ref. [7] to remove the redundant strong phases.

IV. MATRIX ELEMENTS FOR $B^- \to K^- X$ AND $\bar{B}^0 \to K^- X$

We proceed to calculate the matrix elements of the form $< KX|H_{eff}|B >$ which represents the process $B \to KX$ and where H_{eff} has been described above. The effective Hamiltonian consists of operators with a current $\times$ current structure. Pairs of such operators can be expressed in terms of color singlet and color octet structures which lead to color singlet and color octet matrix elements. In the factorization approximation, one separates out the currents in the operators by inserting the vacuum state and neglecting any QCD interactions between the two currents. The basis for this approximation is that, if the quark pair created by one of the currents carries large energy then it will not have significant QCD interactions. In this approximation the color octet matrix element does not contribute because it cannot be expressed in a factorizable color singlet form. The color octet operators could contribute if, for instance, the quark pair emits or absorbs a gluon [21]. It has been shown [20] that in the leading order, where the energy of the light quark pair $E \sim m_b$ with $m_b \to \infty$, the octet matrix element vanishes when the final state is two 0^- mesons. In our case, since the energy of the quark pairs that either creates the K or the X state is rather large, factorization is likely to be a good first approximation. To accommodate some deviation from this approximation we treat N_c, the number of colors that enter in the calculation of the matrix elements, as a free parameter. In our calculation we will see how our results vary with different choices of N_c. The value of $N_c \sim 2$ is suggested by experimental data on low multiplicity hadronic B decays [3].

In the factorization approximation, The matrix element of $B^- \to K^- X$ decay can be expressed as,

$$M = M_1 + M_2 \tag{5}$$

where

$$\begin{aligned}
M_1 &= \frac{G_F}{\sqrt{2}} < K^- \,|\, \bar{s}\gamma^\mu(1-\gamma^5)\, b \,|\, B > \sum_{q=u,d,s} < X \,|\, \bar{q}\, \gamma_\mu \{L_q(1-\gamma^5) + R_q(1+\gamma^5)\}\, q \,|\, 0 > \\
M_2 &= \frac{G_F}{\sqrt{2}} (FL_u < X \,|\, \bar{u}\, \gamma^\mu(1-\gamma^5)\, b \,|\, B >< K^- \,|\, \bar{s}\, \gamma^\mu(1-\gamma^5)\, u \,|\, 0 > \\
&+ FR_u < X \,|\, \bar{u}\, (1-\gamma^5)\, b \,|\, B >< K^- \,|\, \bar{s}\, (1+\gamma^5)\, u \,|\, 0 >)
\end{aligned} \tag{6}$$

where

$$\begin{aligned}
L_u &= V_u \left(c_1 + \frac{c_2}{N_c} \right) + A_3 + \frac{1}{N_c} A_4 + A_9 + \frac{1}{N_c} A_{10} \\
L_d &= A_3 + \frac{1}{N_c} A_4 - \frac{1}{2} \left(A_9 + \frac{1}{N_c} A_{10} \right) \\
L_s &= A_3 + \frac{1}{N_c} A_4 - \frac{1}{2} \left(A_9 + \frac{1}{N_c} A_{10} \right) \\
FL_u &= V_u \left(\frac{c_1}{N_c} + c_2 \right) + \frac{A_3}{N_c} + A_4 + \frac{A_9}{N_c} + A_{10} \\
R_u &= A_5 + \frac{1}{N_c} A_6 + A_7 + \frac{1}{N_c} A_8 \\
R_d &= A_5 + \frac{1}{N_c} A_6 - \frac{1}{2} \left(A_7 + \frac{1}{N_c} A_8 \right) \\
R_s &= A_5 + \frac{1}{N_c} A_6 - \frac{1}{2} \left(A_7 + \frac{1}{N_c} A_8 \right) \\
FR_u &= -2 \left(\frac{1}{N_c} A_5 + A_6 + \frac{1}{N_c} A_7 + A_8 \right)
\end{aligned} \tag{7}$$

We have defined

$$A_i = - \sum_{q=u,c,t} c_i^q V_q \tag{8}$$

with

$$V_q = V_{qs}^* V_{qb} \tag{9}$$

Using the definition

$$< K^- |\, \bar{s}\, \gamma^\mu (1-\gamma^5)\, u \,|\, 0 >= i f_K p_K^\mu \tag{10}$$

where f_K is the kaon decay constant, and the free quark equation of motion one has

$$< K^- |\, \bar{s}\, (1+\gamma^5)\, u \,|\, 0 >= -i \frac{f_K m_K^2}{m_u + m_s} \tag{11}$$

Using these two results we can simplify M_2 and write it in the form

$$M_2 = i f_K [\, \alpha < X \,|\, \bar{u}\, (1+\gamma^5)\, b \,|\, B^- > + \beta < X \,|\, \bar{u}\, (1-\gamma^5)\, b \,|\, B^- >] \tag{12}$$

with

$$\begin{aligned} \alpha &= m_b F L_u \\ \beta &= -m_u F L_u - \frac{F R_u m_K^2}{m_s + m_u} \end{aligned} \tag{13}$$

To calculate M_1 we express

$$< K^- |\, \bar{s}\, \gamma^\mu (1-\gamma^5)\, b \,|\, B >= f_+ (p_B + p_K)^\mu + f_- (p_B - p_K)^\mu \tag{14}$$

where f_+, f_- are Lorentz invariant form factors which are functions of $(p_B - p_K)^2$.

For the decay $\bar{B}^0 \to K^- X$ decay, $M_1 = 0$ and only M_2 contributes.

V. MATRIX ELEMENTS FOR $B^- \to K^{*-} X$ AND $\bar{B}^0 \to K^{*-} X$

For $B^- \to K^{*-} X$ decay, we also write the matrix element as

$$M = M_1 + M_2 \tag{15}$$

where M_1 has a similar structure as in Eq. (6). M_2 has the form

$$M_2 = F L_u < X | \bar{u} \gamma^\mu (1-\gamma^5) b | \bar{B} > m_{K^*} g_{K^*} \varepsilon_\mu^\lambda \tag{16}$$

where

$$< {K^\lambda}^* |\, \bar{s}\, \gamma^\mu (1-\gamma^5)\, u \,|\, 0 >= m_{K^*} g_{K^*} {\varepsilon_\mu}^{\lambda *} \tag{17}$$

with g_{K^*}, the decay constant and ${\varepsilon_\mu}^{\lambda *}$ being the polarisation vector of the vector meson.

For the $\bar{B}^0 \to K^{*-}X$ decay only M_2 contributes. To calculate M_1, following the notation of BSW [25] we write

$$< K^{*-} | \, \bar{s} \, \gamma^\mu (1-\gamma^5) \, b \, | \, B^- > \; = b_1 \varepsilon_{\mu\alpha\beta\gamma} \varepsilon^{\alpha *} p_B^\beta p_{K^*}^\gamma \tag{18}$$

$$+ i \{ b_2 \varepsilon^{\mu *} - b_3 (p_B + p_{K^*})_\mu \varepsilon^* \cdot k + b_4 \varepsilon^* \cdot k k_\mu \} \tag{19}$$

with

$$b_1 = \frac{2V(k^2)}{m_B + m_{K^*}} \tag{20}$$

$$b_2 = (m_B + m_{K^*}) A_1(k^2) \tag{21}$$

$$b_3 = \frac{A_2(k^2)}{m_B + m_{K^*}} \tag{22}$$

$$b_4 = \frac{2 m_{K^*} (A_0(k^2) - A_3(k^2))}{k^2} \tag{23}$$

where $k = p_B - p_{K^*}$. In our calculation we will use the form factors of Ref [26] for the primary result. To check the dependence of the results on form factors we will also use the modified BSW model [27] which has a dipole behavior for the form factors. The form factors in Ref [26] are first evaluated at $k^2 = 0$ and then extrapolated to a finite k^2 assuming a monopole behavior for all the form factors.

We considered the possible contribution from annihilation graphs to both decay rates and asymmetries. In agreement with previous estimates, the annihilation contribution to rates is found to be small [22]. The contribution to CP asymmetries is potentially interesting since the dependence on CKM parameters is quite different. In this case if we limit ourselves to the processes $b \to s u \bar{u}$, $b \to s d \bar{d}$ that have only a strange quark in the $K^{(*)-}$ meson then the contribution to the asymmetry from the annihilation term turns out to be too small to be of interest.

VI. DECAY DISTRIBUTION AND CP ASYMMETRIES

In this section we describe the formalism to calculate the decay distribution, asymmetries and the decay rates.

The general form of the matrix element is

$$M = M_1 + M_2 \tag{24}$$

and so

$$|M|^2 = |M_1|^2 + |M_2|^2 + M_1^\dagger M_2 + M_1 M_2^\dagger \tag{25}$$

Now $|M_1|^2$ has the structure

$$|M_1|^2 = H_{\mu\nu} W^{\mu\nu} \tag{26}$$

where

$$H_{\mu\nu} =< K^-, (K^{*-})|\, J_\mu \,|B^- >< B^- |\, {J_\nu}^\dagger \,|K^-, (K^{*-}) > \tag{27}$$

and

$$W_{\mu\nu} = \sum_X (2\pi)^4 \delta^4(p_B - p_K - p_X) < 0|J_\mu|X >< X|{J_\nu}^\dagger|0 > \tag{28}$$

with

$$J_\mu = \sum_{u,d,s} \bar{q}\gamma_\mu \{L_q(1-\gamma^5) + R_q(1+\gamma^5)\} q \tag{29}$$

In the parton model approximation we can interpret the above process as the decay

$$B(p_B) \to K(p_K) + q(p_1) + \bar{q}(p_2) \tag{30}$$

with $p_X = p_1 + p_2$.

We can also express

$$W_{\mu\nu} = 2Imi \int d^4x e^{-iqx} < 0\,|T(J_\mu(x) J_\nu^\dagger(0))|\,0 > \tag{31}$$

with $q = p_B - p_K = p_X$. The parton model approximation is the leading term in the expansion for the T product in the above equation and so this form for $W_{\mu\nu}$ is useful to calculate higher order corrections to the parton model approximation.

The decay distribution is given by

$$\frac{d\Gamma}{dE_K} = \frac{1}{(2\pi)^3} \frac{1}{16 m_B^2} \int |M_1|^2 dm_{12}^2 \tag{32}$$

where $m_{12}^2 = (p_1 + p_K)^2$ and $|M_1|^2$ has the structure

$$|M_1|^2 = 24 \sum_{u,d,s} [((|L_q|^2 + |R_q|^2) A^1_{\mu\nu} + (|L_q|^2 - |R_q|^2) A^2_{\mu\nu}) H^{\mu\nu} - 2 m_q^2 g_{\mu\nu} H^{\mu\nu} Re(L_q R_q^*)] \tag{33}$$

with

$$\begin{aligned} A^1_{\mu\nu} &= p_{1\mu} p_{2\nu} + p_{1\nu} p_{2\mu} - g_{\mu\nu} p_1 \cdot p_2 \\ A^2_{\mu\nu} &= i\epsilon_{\mu\alpha\nu\beta} p^{2\alpha} p^{1\beta} \qquad (34) \\ & \qquad (35) \end{aligned}$$

(See the Appendix for the full form of $|M_1|^2$.)

For decays involving K^-, $|M_2|^2$ has the form

$$|M_2|^2 = \sum_X \left| < X \mid \bar{u} \left\{ \alpha(1+\gamma^5) + \beta(1-\gamma^5) \right\} b \mid B > \right|^2 (2\pi)^4 \delta^4(p_B - p_K - p_X) \tag{36}$$

$$= \sum_X (2\pi)^4 \delta^4(p_B - p_K - p_X) < B \mid J \mid X >< X \mid J^\dagger \mid B > \tag{37}$$

with

$$J^\dagger = \bar{u}\{\alpha(1+\gamma^5) + \beta(1-\gamma^5)\} b \tag{38}$$

In the parton model approximation we replace

$$\sum_X |X >< X| \to \sum_s \int \frac{d^3p}{(2\pi)^3 2E_u} |u(p_u, s) >< u(p_u, s)| \tag{39}$$

where $|u(p_u, s) >$ is a free quark state with momentum p_u and spin s. As in the previous case it is also possible to express $|M_2|^2$ as

$$|M_2|^2 = 2Im < B|i \int d^4x e^{ip_K x} T(J(x)J^\dagger(0))|B > \tag{40}$$

where the parton model approximation is again the leading term in the expansion of the T product in the above equation and can be interpreted as the two body process $b \to Ku$.

In the parton model approximation we can write for K^- decay,

$$|M_2|^2 = 4f_K^2 \left[(|\alpha|^2 + |\beta|^2) p_b \cdot p_u + 2Re(\alpha\beta^*) m_b m_u \right] \tag{41}$$

and for K^{*-} decay

$$|M_2|^2 = 4|F_{Lu}|^2 m_{K^*}^2 g_{K^*}^2 \left[p_b \cdot p_u + \frac{2p_b \cdot p_{K^*} p_{K^*} \cdot p_u}{M_{K^*}^2} \right] \tag{42}$$

For the interference terms, we have for the K^- decay

$$\begin{aligned} M_1 M_2^\dagger = & -if_K < K^-|\bar{s}\gamma^\mu(1-\gamma^5)b|B > \\ & \sum_X < B|\bar{b}\{\alpha^*(1-\gamma^5) + \beta^*(1+\gamma^5)\}u|X > \\ & < X|\bar{u}\gamma_\mu\{L_u(1-\gamma^5) + R_u(1+\gamma^5)\}u|0 > (2\pi)^4\delta^4(p_B - p_K - p_X) \end{aligned} \tag{43}$$

In the parton model approximation this is written as (using Eq. (39))

$$\begin{aligned} M_1 M_2^\dagger = & -if_K < K^-|\bar{s}\gamma^\mu(1-\gamma^5)b|B > \\ & \int < B|\bar{b}\{\alpha^*(1-\gamma^5) + \beta^*(1+\gamma^5)\}(\not{p}_u + m_u) \\ & \gamma_\mu\{L_u(1-\gamma^5) + R_u(1+\gamma^5)\}u|0 > \frac{d^3p_u}{(2\pi)^3 2E_u}(2\pi)^4\delta^4(p_b - p_K - p_u) \end{aligned} \tag{44}$$

Kinematically this term looks like the two body decay $b \to Ku$.

Using the definition

$$< B^-|\bar{b}\gamma^\mu(1-\gamma^5)u|0 >= if_B p_B^\mu \tag{45}$$

and the quark equation of motion, we have

$$< B^-|\bar{b}(1+\gamma^5)u|0 >= -if_B \frac{m_B^2}{m_b+m_u} \tag{46}$$

and finally we can write (dropping the u quark phase space factor and the delta function)

$$M_1 M_2^\dagger + M_1^\dagger M_2 = 2f_B f_K[ReC\{g_+ p_B \cdot p_u + g_- p_K \cdot p_u\} + ReD\{g_+ m_B^2 + g_- p_B \cdot p_K\}] \tag{47}$$

$$g_+ = f_+ + f_- \tag{48}$$
$$g_- = f_+ - f_- \tag{49}$$
$$C = \frac{2m_B^2}{m_b+m_u}(\alpha^* L_u - \beta^* R_u) \tag{50}$$
$$D = [\beta^* L_u - \alpha^* R_u)]2m_u \tag{51}$$

For decay to K^{*-} one can write a similar expression

$$\begin{aligned} M_1 M_2^\dagger + M_1^\dagger M_2 = {} & 4Re(FL_u^* L_u) m_{K^*} g_{K^*} f_B \sum_i x_i + \\ & 4Re(FL_u^* R_u) m_{K^*} g_{K^*} f_B \frac{m_u m_B^2}{m_b+m_u} \sum_i y_i \end{aligned} \tag{52}$$

where the expressions for x_i, y_i are given in the Appendix .

There will be higher order perturbative corrections, such as additional gluons in the final states, to the processes described above. These effects are expected to be small. We will, however, include the bound state effects of the b quark inside the B meson on the decay distributions .

Inside the B meson, the b quark is not on-shell. This will cause the energy to have a distribution even in the case of "two body" decay. To obtain the decay distribution we consider a model for the B-meson wavefunction [23] which has been used for the calculation of the photon spectrum of inclusive $b \to s\gamma$ decays in Ref. [24].

In the rest frame of the B-meson, the b-quark and the light antiquark $\bar{q}$ inside the B meson with energies E_b and E_q satisfy

$$\begin{aligned} E_b + E_q &= \sqrt{p^2+m_q^2} + \sqrt{p^2+m_b^2} & (53) \\ &= m_B & (54) \end{aligned}$$

where $\vec{p_b} = -\vec{p_{\bar{q}}}, |\vec{p_b}| = p = |\vec{p_{\bar{q}}}|$.

To satisfy Eq. (53) for all p the b-quark mass is considered a function of p,

$$m_b^2 = m_B^2 + m_{\bar{q}}^2 - 2m_B E_q \tag{55}$$

The B-meson wave function is taken as

$$\phi(p) = \frac{4}{\sqrt{\pi}} \frac{1}{p_F^3} e^{-\frac{p^2}{p_F^2}} \tag{56}$$

with the normalization

$$\int_0^\infty p^2 \phi(p) dp = 1. \tag{57}$$

For our numerical results we will use $m_{u,d} = 150$ MeV and the Fermi momentum $p_F = 0.3$ GeV.

The decay distribution is now obtained from

$$\frac{d\Gamma}{dE_K} = \int p^2 dp \phi(p) \left(\frac{d\Gamma}{dE_K} \right)_{partonic} \tag{58}$$

where the partonic distribution $(\frac{d\Gamma}{dE_K})_{partonic}$ can be obtained by boosting the decay distribution in the rest frame of the b-quark to the rest frame of the B-meson.

To complete the numerical calculations we have to fix the value of the gluon momentum q^2 in the G function of Eq. (4). For the "three body" decays governed by $|M_1|^2$, $q^2 = p_X^2$ while for the "two body decay" governed by $|M_2|^2$ and the interference terms one can use simple two body kinematics [28] to obtain $q^2 \approx m_b^2/2$. In our calculation of M_2 we compare results with $q^2 = m_b^2/3$ to those with $q^2 = m_b^2/2$ in order to assess the dependence of the final result on this uncertainty.

Having obtained the decay distributions we define the asymmetry for a B decay,

$$a = \frac{\frac{d\Gamma}{dE_k}(B \to K^{+(*)}X) - \frac{d\Gamma}{dE_k}(\bar{B} \to K^{-(*)}X)}{\frac{d\Gamma}{dE_k}(B \to K^{+(*)}X) + \frac{d\Gamma}{dE_k}(\bar{B} \to K^{-(*)}X)} \tag{59}$$

Integrated decay rates and integrated partial rate asymmetries can also be obtained in the usual manner.

Following Ref [7] we can write the amplitudes, both M_1 and M_2 as

$$\begin{aligned} M_i &= V_u A_u^i + V_c A_c^i + V_t A_t^i \\ &= V_u \Delta_{ut}^i + V_c \Delta_{ct}^i \end{aligned} \tag{60}$$

where $i = 1, 2$ and

$$\begin{aligned} \Delta_{ut}^i &= A_u^i - A_t^i \\ \Delta_{ct}^i &= A_c^i - A_t^i \end{aligned} \tag{61}$$

and the unitarity relation of the CKM, $V_u + V_c + V_t = 0$ has been used. Note that Δ^i_{ut} also contains the tree level amplitude.

The decay distributions are such that the contribution from M_1 and M_2 are separated in E_K in the approximation of neglecting the interference term. The decay distribution is a sum of two independent decay distributions governed by M_1 and M_2. From the structure of M_1 and M_2 it can be seen that the Wilson coefficients that occur in M_1 and M_2 contribute in pairs of the type $c_i + c_{i+1}/N_c$ and $c_{i+1} + c_i/N_c$, respectively. The values of the Wilson's coefficients are such that generally the first combination is suppressed relative to the second and hence M_2 is enhanced relative to M_1. Thus the decay distribution associated with M_2 is larger than the decay distribution associated with M_1.

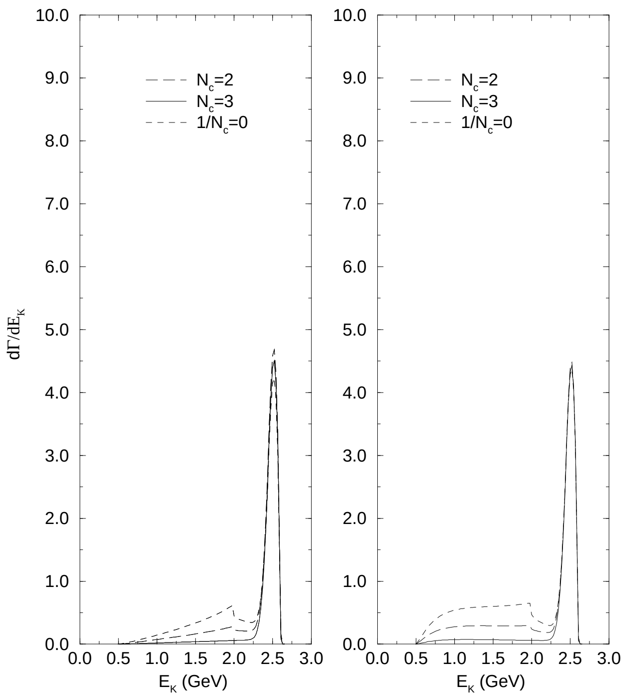

FIG. 3. Predicted Rate for $B^- \to K^- X$ as a function of the kaon energy. Three curves in each figure are shown for $N_c = 2, 3, \infty$ and provide an estimate of the theoretical uncertainty from the factorization hypothesis. In (a) and (b) different sets of form factors are then compared in order to determine the sensitivity of the predicted rate to the choice of a form factor model. The vertical scale in the plots is multiplied by $(G_F/\sqrt{2})^2 \times 10^{-6}$.

Using the form of M_1 and M_2 given above one can write the partial rate asymmetries as

$$a^{ij} = \frac{2Im(V_u{}^* V_c) Im(\Delta^i_{ut} \Delta^{j\,*}_{ct})}{\sum_{ij}\left(|V_u|^2 |\Delta^i_{ut}\Delta^{j\,*}_{ut}| + |V_c|^2 |\Delta^i_{ct}\Delta^{j\,*}_{ct}| + 2Re(V_u{}^* V_c) Re(\Delta^i_{ut}\Delta^{j\,*}_{ct})\right)} \tag{62}$$

where $i, j = 1, 2$. The net asymmetry, a, is given by the sum

$$a = a^{11} + a^{22} + a^{12} + a^{21} \tag{63}$$

From the values of the Wilson coefficients c_1 and c_2 it can be shown that the contribution to the asymmetry due to the interference of the tree and the penguin amplitude is suppressed in a^{11}. This, coupled with the fact that the gluon momentum q^2 is varying for M_1 while it is more or less fixed for M_2 can lead to a larger value for a^{22} compared to a^{11} and a^{12}. It should be pointed out that the interference term between M_1 and M_2 can be important when calculating the partial rate asymmetries.

VII. RESULTS AND DISCUSSION OF THEORETICAL UNCERTAINTIES

In this section we discuss the results of our calculations which are shown graphically in Figs. 3-20. We find that there can be significant asymmetries in $B \to K(K^*)X$ decays especially in the region $E_K > 2$ GeV which is also the region where an experimental signal for such decays can be isolated. The branching ratios are of order $O(10^{-4})$ which are within reach for future B factories.

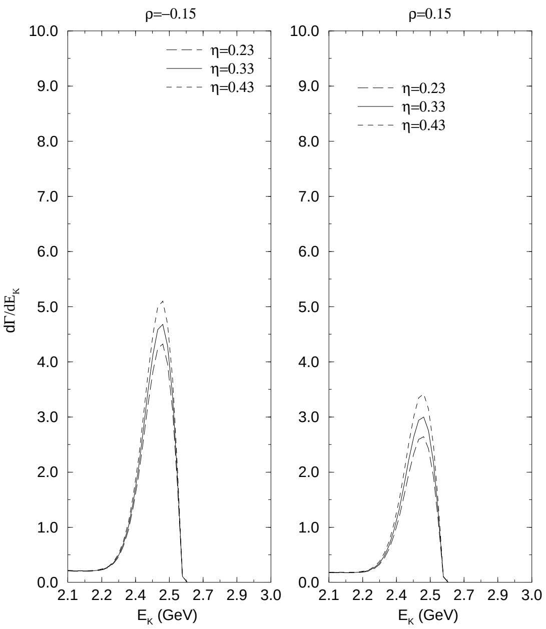

FIG. 4. Sensitivity of the predicted rate for $B^- \to K^- X$ to ρ, η. The three curves indicate the sensitivity of the rate to the value of Wolfenstein parameter η for fixed values of ρ

The contribution of the amplitude with the top quark in the loop accounts for 60-75% of the inclusive branching fraction. However, since the top quark amplitude is large and has no absorptive part in contrast to the c quark amplitude, the top quark contribution reduces the net CP asymmetry from 30-50% to about 10%. This calculation includes the contribution from electroweak penguins. We find that the electroweak penguin contributions increase the decay rates by 10-20% but reduce the overall asymmetry by 20-30%.

Let us now identify the main sources of uncertainties in our calculation. These are the use of the factorization approximation, the choice of a form factor model, the choice of q^2 for the gluon

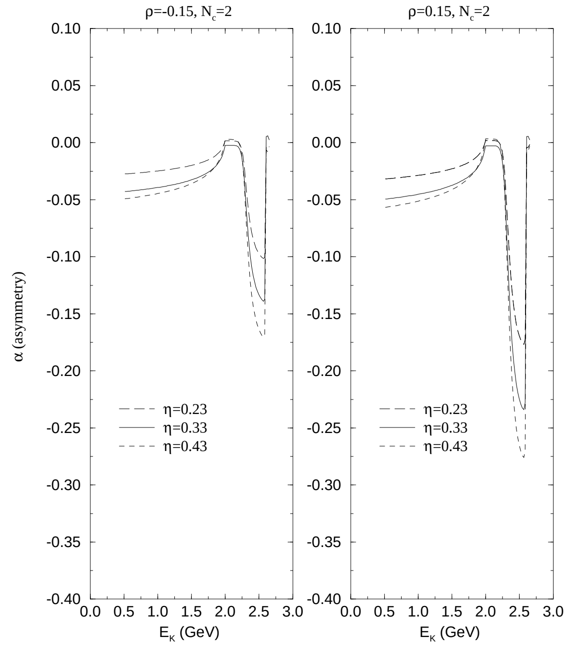

FIG. 5. Sensitivity of the asymmetry for $B^- \to K^- X$ to the parameter Wolfenstein parameter η for two fixed values of ρ. The three curves indicate the sensitivity of the asymmetry as a function of kaon energy.

momentum in the G function in Eq. (4) for the "internal" two body diagrams, and the choice of a model for the B-meson. We now discuss the sensitivity of the results for decay rates and asymmetries to these theoretical uncertainties.

We have used the factorization approximation. The factorization approximation is expected to be valid in our calculations as we have argued at the beginning of Section 2. To take into account corrections to this approximation we allowed the number of colors to be a free parameter. In our calculation we consider the cases $N_c = 2,\ 3,\ \infty$ although the analysis of exclusive two body B decays suggests that $N_c \sim 2$. In Fig. 3 we show the decay distribution for $B^- \to K^- X$ where X does not contain any strange particles. In the region of interest to experiment (i.e $E_K > 2.0$ GeV) the decay distribution has only a modest dependence on N_c.

The second source of uncertainty is the choice of form factors used to describe the $B \to K(K^*)$ transitions. As mentioned earlier we use the form factors given in Ref. [26]. In Ref [26] a monopole k^2 dependence for the form factors is chosen and the form factor at $k^2 = 0$ for the D decays is fixed from semileptonic $D \to K$ decays. The form factors are then scaled to the case of $B \to K$ decay using HQET. The primary effect of choosing a different set of form factors in our calculations is to change the decay distribution of the "three body distribution" which is governed by the matrix element M_1. Figs. 3(a), 3(b) show the effect of choosing two sets of form factors from Ref [26] and Ref [27] with a different k^2 behavior of the form factors. For the energy region $E_K > 2$ GeV the form factor effects are negligible for the decay distributions as well as the asymmetries. For the remainder of the discussion and in the rest of the figures we will only show the results with form factors from Deandrea et al. [26].

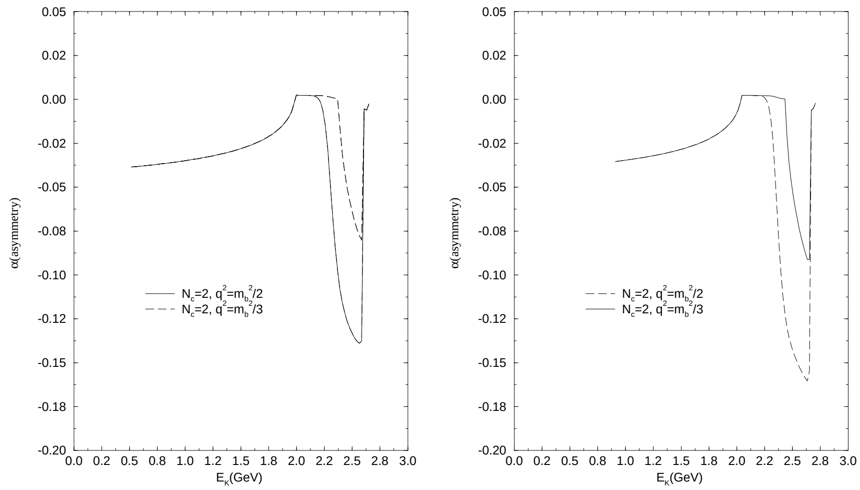

FIG. 6. Predicted Asymmetries for $B^- \to K^- X$ and $B^- \to K^{*-} X$ as a function of the kaon energy. The value of $N_c = 2$ is fixed. The two sets of curves indicate the sensitivity of the asymmetry to the values of q^2 for the gluon in the internal two body diagram.

The asymmetries are sensitive to the values of the Wolfenstein parameters ρ and η. The existing constraints on the values of ρ and η come from measurements of $|V_{ub}|/|V_{cb}|$, ϵ_K in the K system and ΔM_{B_d}. (See Ref. [29] for a recent review). In our calculation we will use $f_B = 170$ MeV and choose $(\rho = -0.15, \eta = 0.33)$. To determine the dependence of our results on η we will also consider three sets of representative values, $(\rho = -0.15, \eta = 0.23)$, $(\rho = -0.15, \eta = 0.33)$ and $(\rho = -0.15, \eta = 0.43)$. We will also consider the set of η values with $\rho = 0.15$. The dependence of the rates on ρ, η is shown in Fig. 4, while the sensitivity of the asymmetry to these parameters is shown in Fig. 5. For fixed ρ, the asymmetry increases monotonically as η increases. The results suggest that measurement of asymmetries in inclusive decays will give useful information on η once the size of the theoretical uncertainties is reduced.

There are several other sources of uncertainty. These are: (1) the choice of q^2 for the gluon momentum in the G function in Eq. (4) for the "internal" two body diagrams and (2) the choice of a model for the wavefunction of the B-meson. The q^2 variation causes a small change in the decay distribution but a fairly significant change in the asymmetries. This uncertainty is illustrated by comparison of the two curves in Figs. 6, 15.

The choice of the value of the charm quark mass m_c, is also a source of uncertainty for the asymmetry. We have taken $m_c = 1.35$ GeV for this calculation. Increasing the charm quark mass to $m_c = 1.6$ GeV does not significantly modify the decay rates but reduces the asymmetry by about 30%. Since the Wilson coefficients are calculated to next to leading order, they are insensitive to the renormalization scale. However, the G function which enters into the calculation does have a dependence on renormalization scale. Varying μ^2 from $m_b^2/2$ to $2m_b^2$ changes both the asymmetry and the decay rates by $\pm 10\%$. A lower renormalization scale corresponds to a larger asymmetry. The model of the B meson wavefunction, used to take into account the Fermi motion of the quarks, is yet another source of uncertainty. We have used the model of Ali et al. which has been previously used

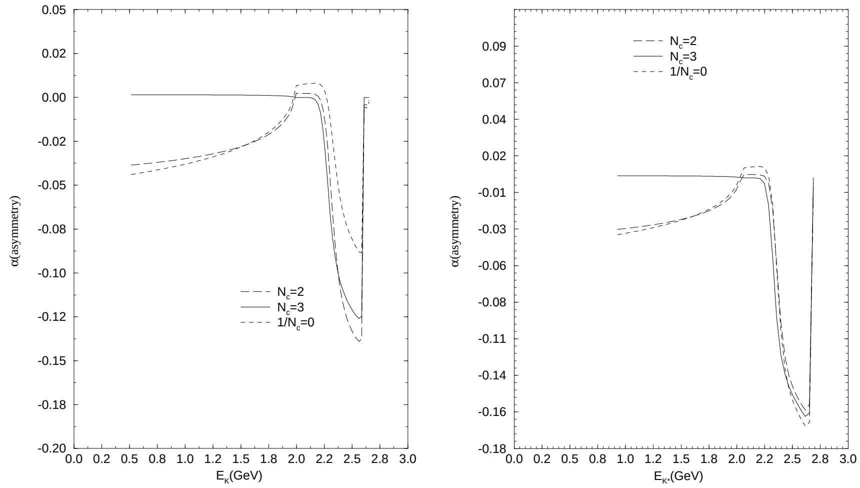

FIG. 7. Predicted Asymmetries for $B^- \to K^- X$ and $B^- \to K^{*-} X$ as a function of the kaon energy. The three sets of curves indicate the sensitivity of the asymmetry to the value of N_c. The values $N_c = 2, 3, \infty$ are considered.

for the $B \to X_s \gamma$ case. Different models give somewhat different results for the decay distributions while the asymmetries are insensitive to the choice of model for the B meson wavefunction.

In Fig. 8 we show the decay distribution for K^* in the final state while in Figs. 14, 13 we show the variation of the decay distribution and asymmetry with different sets of ρ, η for $N_c = 2$. In Fig. 11 we show the asymmetry for several values of N_c using the form factors from Ref [26] and $q^2 = m_b^2/2.0$. A similar variation of the asymmetry with q^2 as calculated for the K in the final state is also observed in this case as shown in Fig. 10.

Turning to B^0 decays, only the M_2 part of the matrix element contributes. In Fig. 11 we show the decay distribution for various N_c values using the form factors from Ref [26] and $q^2 = m_b^2/2.0$. In Fig. 12 we show the decay distributions of $\bar{B}^0 \to K^-$ for representative values of (ρ, η). In Figs. 14, 15 we show the asymmetries as we vary (ρ, η) and q^2. The variation of the asymmetries with N_c is negligible in this case.

In Table. I we give the branching fractions and the integrated asymmetries for the inclusive decays for different N, $q^2 = m_b^2/2$, $f_B = 170$ MeV, $\rho = -0.15, \eta = 0.33$ and the form factors from Ref. [26]. For the charged B decays we also show the decay rates and asymmetries for $E_K > 2$ (2.1) GeV as that is the region of the signal.

The above figures show that there can be significant asymmetries in $B \to K^{(*)} X$ decays, especially in the region $E_K > 2$ GeV which is the region of experimental sensitivity for such decays. As already mentioned, our calculation is not free of theoretical uncertainties. Two strong assumptions used in our calculation are the use of quark level strong phases for the FSI phases at the hadronic level and the choice of the value of the gluon momentum q^2 in the two body decays. Other uncertainties from the use of different heavy to light form factors, the use of factorization, the model of the B meson wavefunction, the value of the charm quark mass and the choice of the renormalization

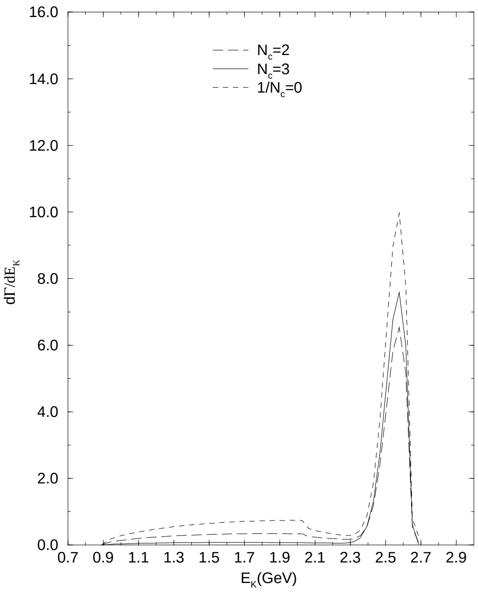

FIG. 8. Predicted Rate for $B^- \to K^{*-}X$ as a function of the kaon energy. The three curves indicate the sensitivity of the rate to the value of N_c. The values $N_c = 2, 3, \infty$ are considered.

scale μ have smaller effects on the asymmetries.

VIII. COMPARISON WITH PREVIOUS CALCULATIONS

Inclusive direct CP violating asymmetries were calculated by Gerard and Hou [7]. They obtained asymmetries much smaller than the results given here. The differences between these calculations and our results can be understood as follows. In the Gerard-Hou calculation only the three body quark level process corresponding to $b \to sq\bar{q}$ (i.e. M_1 in equation (1)) was considered and the limit $N_c \to \infty$ was taken. With these conditions we obtain an asymmetry of -1.7% which then agrees with their result. We obtain large asymmetries only in the kinematic regime dominated by two-body process $b \to K\ u$. These asymmetries agree qualitatively with the asymmetry for exclusive modes such as $B^- \to K^-\pi^0$ found in several recent calculations in both sign and magnitude. In the kinematic region of $B^- \to K^-\pi^0$ we find an asymmetry of $-(8-14)\%$ to be compared with and $-(2-8)\%$ found by Kramer, Palmer, and Simma [12] and $-(3-9)\%$ found by Kamal and Luo [11] for the exclusive mode $B^- \to K^-\pi^0$.

We have also verified that the asymmetry in the process $b \to sc\bar{c}$ has the opposite sign to the asymmetry in the sum of $b \to su\bar{u}$, $b \to sd\bar{d}$, $b \to ss\bar{s}$ (as does the asymmetry in $B \to D\bar{D}$) as required by CPT to insure the cancellation between all modes.

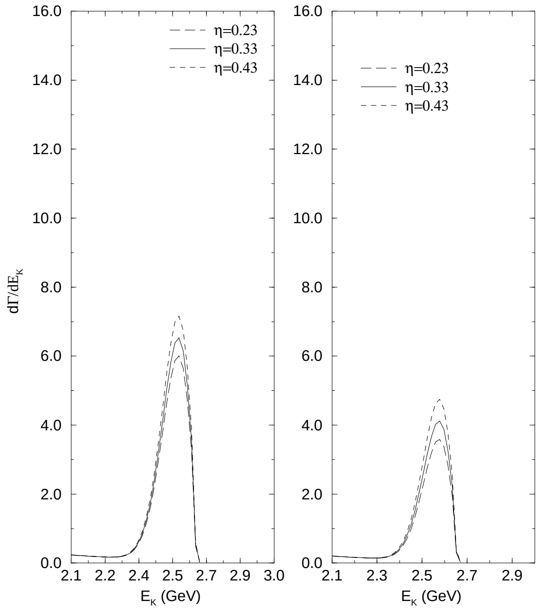

FIG. 9. Predicted Rate for $B^- \to K^{*-}X$ as a function of the kaon energy. The three curves indicate the sensitivity of the rate to the values of Wolfenstein parameters ρ, η. Only the signal region is shown in the figures.

IX. CONCLUSION

We find significant direct CP violation in the inclusive decay $B \to K^- X$ and $B \to K^{*-} X$ for $2.7 > E_{K^{(*)}} > 2.0$ GeV. The branching fractions are in the 10^{-4} range and the CP asymmetries may be sizeable. These asymmetries should be observable at future B factories and could be used to rule out the superweak class of models.

X. ACKNOWLEDGEMENTS

We thank K. Berkelman, W-S. Hou, A. Kagan, L. Wolfenstein, and H. Yamamoto for useful discussions and comments. This work was supported by the Australian Research Council and by the United States Department of Energy under contracts DE-FG 02-92ER10730 and DE-FG 03-94ER40833. X.-G. He thanks the University of Iowa and the University of Oregon for hospitality during the preparation of this work.

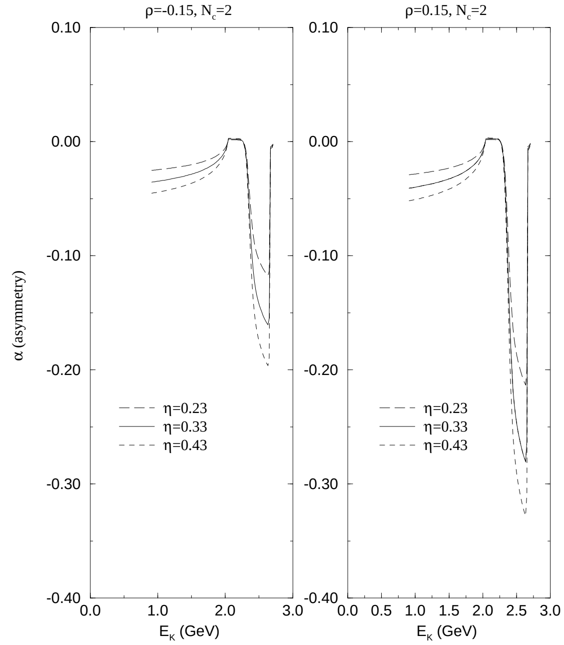

FIG. 10. Predicted Asymmetry for $B^- \rightarrow K^{*-}X$ as a function of the kaon energy. The three curves indicate the sensitivity of the asymmetry to the values of Wolfenstein parameters $\rho,\ \eta$.

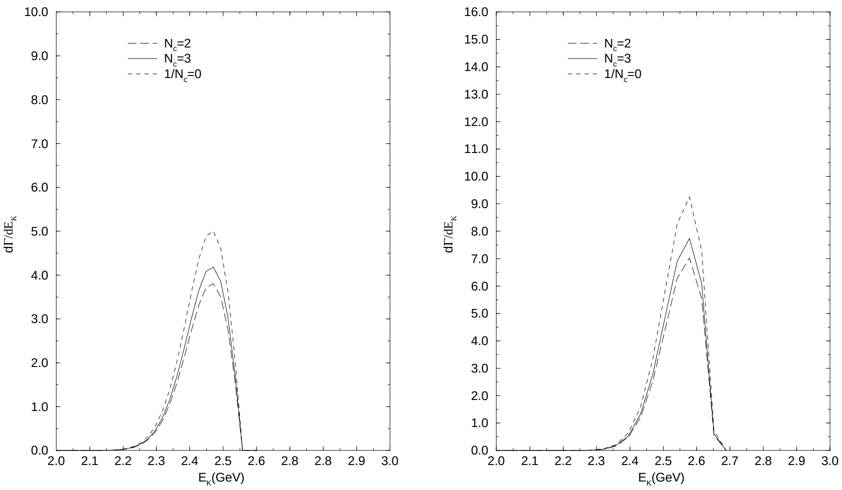

FIG. 11. Predicted Rate for $\bar{B}^0 \rightarrow K^-X$ and $\bar{B}^0 \rightarrow K^{*-}X$ as a function of the kaon energy. The three sets of curves indicate the sensitivity of the rate to the value of N_c. The values $N_c = 2, 3, \infty$ are considered.

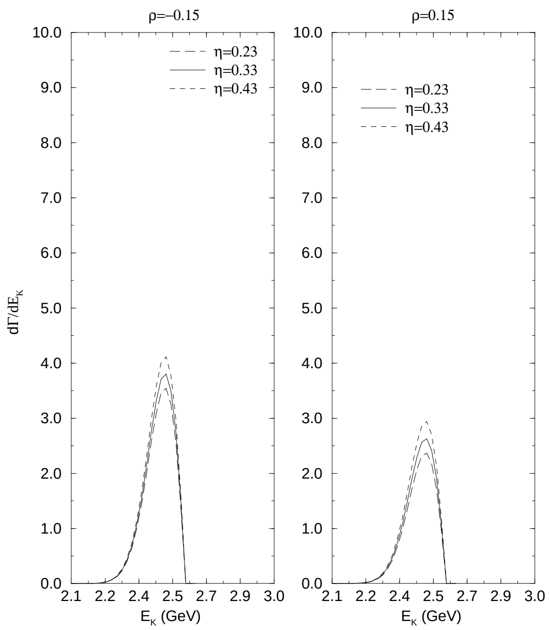

FIG. 12. Predicted Rate for $\bar{B}^0 \to K^- X$ as a function of the kaon energy. The three curves indicate the sensitivity of the rate to the values of Wolfenstein parameters $\rho,\ \eta$.

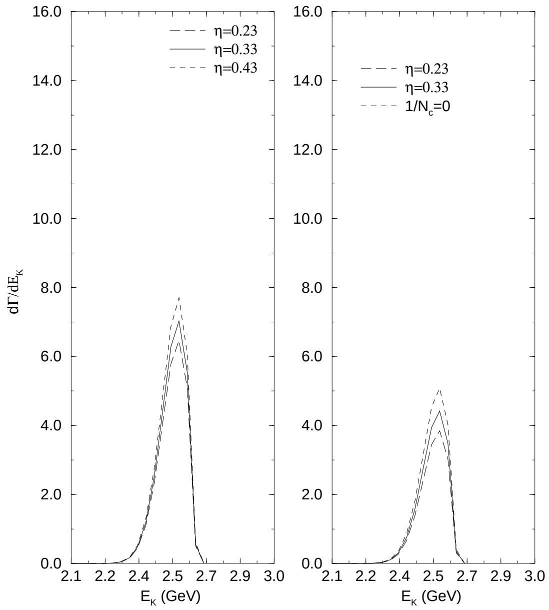

FIG. 13. Predicted Rate for $\bar{B}^0 \to K^{*-} X$ as a function of the kaon energy. The three curves indicate the sensitivity of the rate to the values of Wolfenstein parameters $\rho,\ \eta$.

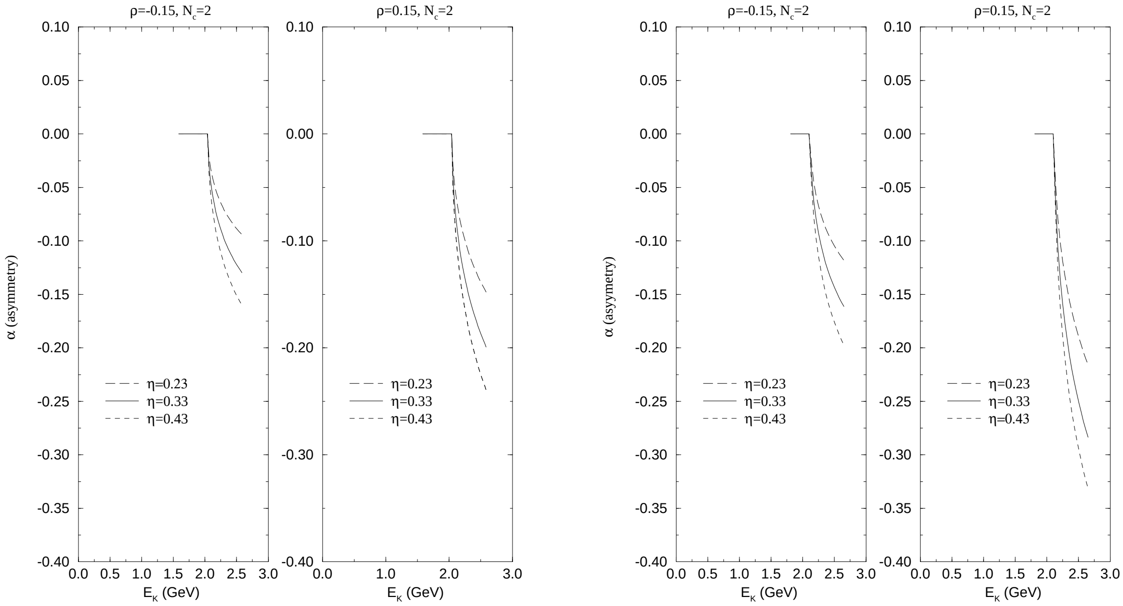

FIG. 14. Predicted Asymmetries for $\bar{B}^0 \to K^- X$ and $\bar{B}^0 \to K^{*-} X$ as a function of the kaon energy. The three curves in each figure indicate the sensitivity of the rate to the values of Wolfenstein parameters $\rho,\ \eta$.

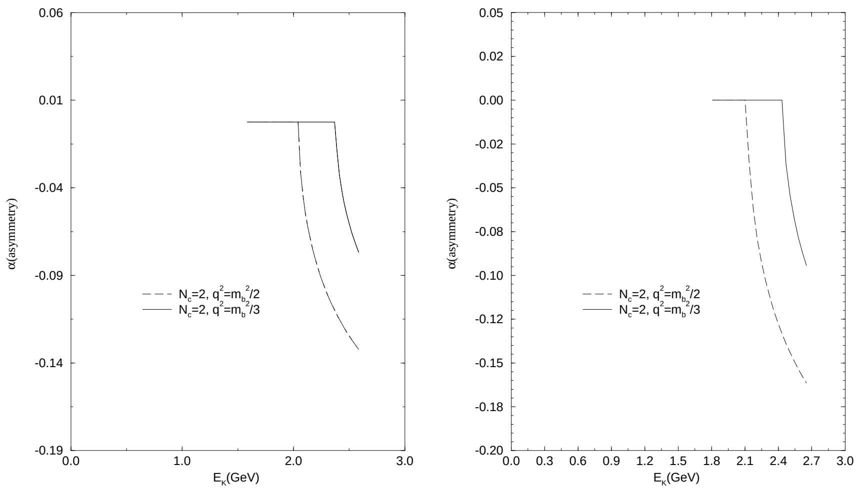

FIG. 15. Predicted Asymmetries for $\bar{B}^0 \to K^- X$ and $\bar{B}^0 \to K^{*-} X$ as a function of the kaon energy. The two sets of curves indicate the sensitivity of the asymmetry to the values of q^2 for the gluon in the internal two body diagram.

TABLE I. Integrated decay rates and asymmetries for $B \to K^{(*)}X$ Decay

Process	Branching Ratio (1.65×10^{-4})	Integrated Asymmetry
$B^- \to K^- X$	$1.02, 0.79, 1.20$	$-0.10, -0.11, -0.050$
$B^- \to K^- X (E_K > 2.1\mathrm{GeV})$	$0.81, 0.74, 0.77$	$-0.12, -0.12, -0.07$
$\overline{B}^0 \to K^- X \ (E_K > 2.1\mathrm{GeV})$	$0.6, 0.7, 0.8$	$-0.12, -0.12, -0.13$
$B^- \to K^{*-} X$	$1.37, 1.24, 2.30$	$-0.11, -0.14, -0.11$
$B^- \to K^{*-} X (E_{K^*} > 2.1\mathrm{GeV})$	$1.05, 1.16, 1.67$	$-0.14, -0.15, -0.14$
$\overline{B}^0 \to K^{*-} X \ (E_{K^*} > 2.1\mathrm{GeV})$	$1.05, 1.16, 1.39$	$-0.15, -0.15, -0.16$

XI. APPENDIX

For $B^- \to K^- X$ decay

$$A^1{}_{\mu\nu} H^{\mu\nu} = |g_+|^2 D(p_B, p_B) + |g_-|^2 D(p_K, p_K) + 2Re(g^+ g_-^*) D(p_B, p_K) \tag{64}$$
$$A^2{}_{\mu\nu} H^{\mu\nu} = 0 \tag{65}$$

where

$$\begin{aligned} g_+ &= f_+ + f_- \\ g_- &= f_+ - f_- \end{aligned} \tag{66}$$

and we have defined

$$D(A, B) = A \cdot p_1 \, B \cdot p_2 + B \cdot p_1 \, A \cdot p_2 - p_1 \cdot p_2 \, A \cdot B \tag{67}$$

$$g_{\mu\nu} H^{\mu\nu} = |g_+|^2 m_B^2 + |g_-|^2 m_K^2 + 2Re(g_+ g_-^*) \, p_B \cdot p_K \tag{68}$$

For $B^- \to K^{*-} X$ decays (with $p = p_B + p_{K^*}, q = p_B - p_{K^*}$),

$$H^{\mu\nu} A^1{}_{\mu\nu} = \sum T_i \tag{69}$$

$$\begin{aligned} T_1 &= b_1^2[-2p_1 \cdot p_2 (m_B^2 m_{K^*}^2 - (p_B \cdot p_{K^*})^2) \\ &\quad +2p_B \cdot p_{K^*} D(p_B, p_{K^*}) - {m_{K^*}}^2 D(p_B, p_B) - m_B^2 D(p_{K^*}, p_{K^*})] \\ T_2 &= b_2^2 \left[2p_1 \cdot p_2 + \frac{1}{m_{K^*}^2} D(p_{K^*}, p_{K^*}) \right] \\ T_3 &= b_3^2 F D(p, q) \\ T_4 &= b_4^2 F D(p, q) \\ T_5 &= 2b_2 b_3 [D(q, p) - x D(p_{K^*}, p)] \\ T_6 &= 2b_2 b_4 [-D(q, q) + x D(q, p_{K^*})] \\ T_7 &= -2F b_3 b_4 D(p, q) \end{aligned} \tag{70}$$

while

$$H^{\mu\nu} A^2{}_{\mu\nu} = 4c_1 c_2 [p_1 \cdot p_B p_2 \cdot p_{K^*} - p_2 \cdot p_B p_1 \cdot p_{K^*}] \tag{71}$$
$$\tag{72}$$

and

$$g_{\mu\nu} H^{\mu\nu} = \sum S_i \tag{73}$$

$$
\begin{aligned}
S_1 &= -2b_1^2[m_{K^*}^2 m_B^2 - (p_B \cdot p_{K^*})^2] \\
S_2 &= -3b_2^2 \\
S_3 &= Fb_3^2 p^2 \\
S_4 &= b_4^2 q^2 \\
S_5 &= 2b_2 b_3[q \cdot p - x p_{k^*} \cdot p] \\
S_6 &= 2b_2 b_4[-q^2 + xp \cdot q] \\
S_7 &= -2Fb_3 b_4 p \cdot q
\end{aligned} \tag{74}
$$

where

$$
\begin{aligned}
F &= \left[-q^2 + \frac{(p_{K^*} \cdot q)^2}{m_{K^*}{}^2}\right] \\
x &= \frac{p_{K^*} \cdot q}{m_{K^*}{}^2}
\end{aligned} \tag{75}
$$

Finally for K^* decay the interference term is with $p_1 = p_B$, $p_2 = p_{K^*}$ and $q = p_1 - p_2$

$$
\begin{aligned}
x_1 &= 2b_1[m_B^2 p_u \cdot p_2 - p_1 \cdot p_u p_2 \cdot p_1] \\
x_2 &= -b_2 \left[2p_1 \cdot p_u + \frac{D(p_2, p_2)}{M_2^2}\right] b \\
x_3 &= -b_3 \left[D(p_1 + p_2, q) - \frac{p_2 \cdot q}{M_2^2} D(p_1 + p_2, p_2)\right] \\
x_4 &= -b_4 \left[-D(q, q) + \frac{p_2 \cdot q}{M_2^2} D(q, p_2)\right] \\
y_1 &= -3b_2 \\
y_2 &= b_3[(p_1 + p_2) \cdot q - (p_1 + p_2) \cdot p_2 \frac{p_2 \cdot q}{M_2^2}] \\
y_3 &= b_4[q^2 - q \cdot p_2 \frac{p_2 \cdot q}{M_2^2}] \\
D(A, B) &= A \cdot p_1 \, B \cdot p_u + A \cdot p_u \, B \cdot p_B - p_u \cdot p_1 \, A \cdot B
\end{aligned} \tag{76}
$$

REFERENCES

[1] D. Boutigny et al., *Letter of Intent for the Study of CP Violation and Heavy Flavor Physics at PEPII*, SLAC Report-0443, The BABAR collaboration, 1994.

[2] K. Abe et al., *Physics and Detector of Asymmetric B Factory at KEK*, KEK Report 90-23 (1991). Also see *Letter of Intent for A Study of CP Violation in B Meson Decays*, KEK Report 94-2, April 1994.

[3] For a review see A. Ali, hep-ph/96010, M. Gronau, TECHNION-PH-96-39, hep-ph/9609430; T.E. Browder and K. Honscheid, Progress in Nuclear and Particle Physics, Vol. 35, ed. K. Faessler, p. 81-220 (1995).

[4] A. Buras, hep-ph/9509329 and Nucl. Instrum. Meth. **A 368**, 1 ,1995; J. L. Rosner, hep-ph/9506364 and Proceedings of the 1995 Rio de Janeiro School on Particles and Fields, 116; A. Ali and D. London, DESY 95-148, UDEM-GPP-TH-95-32, hep-ph/9508272.

[5] N. G. Deshpande, X.-G. He and S. Oh, hep-ph/9511462; M. Gronau, hep-ph/9609430 and Nucl. Instrum. Meth. **A 384**, 1, 1996; R. Fleischer, hep-ph/9612446, to appear in Int. J. Mod. Phys. A.

[6] M. Bander, D. Silverman and A. Soni, Phys. Rev. Lett. **43** 242 (1979).

[7] J. Gerard and W.-S. Hou, Phys. Rev. Lett. **62**, 855 (1989); J. Gerard and W.-S. Hou, Phys. Rev.**D 43**, 2909 (1991), H. Simma, G. Eilam and D. Wyler, Nucl. Phys. **B 352**, 367 (1991);

[8] L. Wolfenstein, Phys. Rev.**D 43**, 151 (1991).

[9] R. Fleischer, Z. Phys. **C 58** 438; Z. Phys. **C 62** 81; G. Kramer, W. F. Palmer and H. Simma, Nucl. Phys. **B 428** 77 (1994); Z. Phys. **C 66** 429, (1994); N.G. Deshpande and X.-G. He, Phys. Lett. **B 336**, 471 (1994).

[10] D.-S. Du and Z.-Z. Xing, Z. Phys. **C 66**, 129, (1995).

[11] A.N. Kamal and C.W. Luo, hep-ph/9612401, Alberta-THY-43-96.

[12] G. Kramer,W.F. Palmer, and H. Simma, Z. Phys. **C 66**, 429, (1995).

[13] J.P. Silva and L. Wolfenstein, Phys. Rev. **D 55**, 5331 (1997) and references therein.

[14] M.S. Alam et al. (CLEO Collaboration), Phys. Rev. Lett. **74**, 2885 (1995).

[15] K. W. Edwards et al. (CLEO Collaboration), CLEO CONF 95-8.

[16] P.C. Kim (CLEO Collaboration) contribution to the Proceedings of the FCNC97 conference, J. Alexander and B. Behrens (CLEO Collaboration), contribution to the Proceedings of the BCONF97 conference.

[17] M. Lautenbacher and P. Weisz, Nucl. Phys. **B 400**, 37 (1993); A. Buras, M. Jamin and M. Lautenbacher, ibid, 75 (1993); M. Ciuchini, E. Franco, G. Martinelli and L. Reina, Nucl. Phys. **B 415**, 403(1994).

[18] J. Gasser and H. Leutwyler, Phys. Rep. **87**, 77 (1982).

[19] K. Hikasa et al. (Particle Data Group), Phys. Rev.**D 54**, 303 (1996).

[20] J. F. Donoghue and A. A. Petrov, Phys. Lett. **B 393**, 149, 1997.

[21] P. Ko, J. Lee and H.S. Song, Phys. Rev. **D53**, 1409 (1996); X.-G. He and A. Soni, Phys. Lett. **B 391**, 456, 1997.

[22] M. Gronau, O. F. Hernandez, D. London, J. L. Rosner, Phys. Rev. **D 50**, 4529 (1994).

[23] A. Ali and E. Pietarinen, Nucl. Phys. **B 154**, 519 (1979); G. Altarelli *et al.*, Nucl. Phys. **B 208**, 365 (1982).

[24] A. Ali and C. Greub, Z. Phys. **C 49**, 431 (1991).
[25] M. Bauer, B. Stech and M, Wirbel, Z. Phys. **C 34**, 103 (1987);
[26] R. Casalbouni *et al.*, Phys. Lett. **299**, 139 (1993); A. Deandrea, N. Di Bartolomeo, R. Gatto, and G. Nardulli, Phys. Lett. **B 318**, 549 (1993).
[27] M. Neubert, V. Riekert, Q.P. Xu, and B. Stech, in *Heavy Flavors*, edited by A.J. Buras and H. Lindner (World Scientific, Singapore, 1992).
[28] N.G. Deshpande and J. Trampetic, Phys. Rev. **D 41**, 895 (1990); N. G. Deshpande, "Theory of Penguins in B decays", in B Decays ed. S. Stone, (World Scientific, Singapore, 1994)
[29] A. Ali and D. London, Nucl. Phys. Proc. Suppl. **54 A**, 29, 1997, also hep-ph/9607392.